Hydrol. Earth Syst. Sci. Discuss., 10, 10997–11033, 2013
www.hydrol-earth-syst-sci-discuss.net/10/10997/2013/
doi:10.5194/hessd-10-10997-2013

Hydrology and Earth System Sciences
Open Access
Discussions

Using globally available soil moisture indicators for flood modelling in Mediterranean catchments

C. Massari[1], **L. Brocca**[1], **S. Barbetta**[1], **C. Papathanasiou**[2], **M. Mimikou**[2], **and T. Moramarco**[1]

[1]Research Institute for Geo-Hydrological Protection, National Research Council, Perugia, Italy
[2]Laboratory of Hydrology and Water Resources Management,
National Technical University of Athens, Athen, Greece

Received: 23 July 2013 – Accepted: 16 August 2013 – Published: 22 August 2013

Correspondence to: C. Massari (christian.massari@irpi.cnr.it)

Published by Copernicus Publications on behalf of the European Geosciences Union.

Abstract

Floods are one of the most dangerous natural hazards in Mediterranean regions. Flood forecasting tools and early warning systems can be very beneficial to reduce flood risk. Event-based rainfall runoff models are frequently employed for operational flood forecasting purposes because of their simplicity and the reduced number of parameters involved with respect to continuous models. However, the advantages that are related with the reduced parameterization face against the need for a correct initialization of the model, especially in areas affected by strong climate seasonality. On the other hand, the use of continuous models may be very problematic in poorly gauged areas. This paper introduces a simplified continuous rainfall-runoff model, which uses globally available soil moisture retrievals to identify the initial wetness condition of the catchment, and, only event rainfall data to simulate discharge hydrographs. The model calibration involves only 3 parameters. For soil moisture, beside in situ and modelled data, satellite products from the Advanced SCATterometer (ASCAT) and the Advanced Microwave Scanning Radiometer for Earth observation (AMSR-E) sensors are employed. Additionally, the ERA-LAND reanalysis soil moisture product of the European Centre for Medium Range Weather Forecasting (ECMWF) is used.

The model was tested in the small catchment of Rafina, 109 km^2 located in the Eastern Attica region, Greece. Specifically, fifteen rainfall-runoff events were modelled by considering different configurations for the initial soil moisture conditions. Comparing the performance of the different soil moisture products, it was found that all global indicators allow reproducing fairly well the selected flood events providing much better results than the situation where a constant initial condition is provided. ERA-LAND slightly outperforms the satellite soil moisture products and in general, all the indicators give the same performance obtained by ground and continuously simulated soil moisture data. Due to the wide diffusion of globally available soil moisture retrievals and the small amount of parameters used, the proposed modelling approach is very suitable for runoff prediction in poorly gauged areas.

1 Introduction

In the context of climate change, in which runoff production mechanisms appear to be exacerbated by the modification of climatic variables, the flood frequency regime is altered and an increasing frequency of extreme events is to be expected. The Report of Intergovernmental Panel on Climate Change (IPCC, 2001) on potential effects of climate change highlights that "flood magnitude and frequency are likely (a 66–90 % probability) to increase in most regions". Notwithstanding this issue, Europe seems to lack suitable and reliable procedures to promptly address the fundamental issues of flood-risk assessment and management Even though several important laws and directives have been issued addressing this point, i.e. European Floods Directive 2007/60/CE, these legislative tools have not succeeded yet in effectively reducing the devastating and catastrophic effects of extreme flood events (Barredo, 2006). To this end, flood forecasting and early warning systems have been identified as fundamental tools for the prevention and the protection from flood risk.

The development of an early warning system for flood forecasting is particularly difficult for small to medium sized basins (area $< 400\,\mathrm{km}^2$) for which the hydrologic response is extremely fast and an hourly (or finer) temporal resolution for datasets is required (Younis et al., 2008). To accomplish this task, a rainfall-runoff (RR) model able to simulate not only the runoff formation process (i.e. estimation of losses) but also the hydrological routing along hillslopes and channels has to be set up. Besides the spatial discretization (lumped versus distributed models) and the process description (physically-based versus conceptual models), RR models applied for operational flood forecasting can be subdivided in two main categories: continuous and event-based (Brocca et al., 2011; Paquet et al., 2013). On one hand, continuous RR models simulate the temporal evolution of the soil wetness conditions of the catchment thus being able to model the complex interaction between rainfall and soil moisture (SM) conditions needed to properly predict flood hydrographs (Camici et al., 2011). However, the different processes (infiltration, percolation, evapotranspiration, interception) involved in the simulation of the SM temporal evolution may require a large number of parameters to be identified. This could easily introduce significant uncertainties into the model prediction and non identifiably problems (Beven, 2006). Moreover, continuous models require long-term and uninterrupted time series for the input data (e.g. rainfall and temperature) and this could be a strong limitation in many regions worldwide, mainly if hourly observations are needed (Viviroli et al., 2009). On the other hand, event-based RR models need a reduced parameterization, and they are easy to be applied even from users without a strong hydrological expertise and require a low computational effort. For that, this type of models are very appealing, and frequently employed within operational flood forecasting systems (Coustau et al., 2012). The major limitations of event-based models lie in the definition of the initial SM conditions that could be very different from one storm event to another (Tramblay et al., 2012; Coustau et al., 2012, Van Steenbergen and Willems, 2013). This issue is particularly challenging in regions characterized by strong seasonality of the climate as it occurs in Mediterranean basins (Aronica and Candela, 2004).

Nowadays, several SM data sources are available, also at a global scale. Specifically, SM information can be obtained from in situ and satellite sensors or from land surface models. From in situ observations, it is worth mentioning the International Soil Moisture Network (Dorigo et al., 2011) that is an international cooperation to establish and maintain a global in situ SM database that can be used for global analysis e.g. the validation of the retrieval algorithms applied to remote sensing observations. Moreover, several satellite SM products are globally and freely available from active and passive microwave sensors, e.g. the Advanced SCATterometer, ASCAT (Bartalis et al., 2007), the Advanced Microwave Scanning Radiometer for Earth observation, AMSR-E (Owe et al., 2008), the Microwave Imaging Radiometer with Aperture Synthesis, MIRAS (Kerr et al., 2010). The accuracy and maturity of these satellite products contributed to the implementation of a fully operational near-real-time (NRT) SM processing chain for ASCAT (Wagner et al., 2013) from the European Organisation for the Exploitation of Meteorological Satellites (EUMETSAT) since December 2008. Finally, modelled SM data obtained from numerical weather prediction systems operated by international meteorological centres (e.g. the ECMWF, European Centre for Medium Range Weather Forecasting) are also available at a global scale. As an example, in the context of EUMETSAT's H-SAF project (Satellite Application Facility on Support to Operational Hydrology and Water Management), an ASCAT root zone SM profile product has been developed based on ASCAT surface SM data assimilation into the ECMWF Land Surface Data Assimilation System (De Rosnay et al., 2013). All these SM datasets, which are globally available, might be potentially used for the initialization of event-based RR models in different catchments and regions worldwide even for poorly gauged areas.

Some studies attempted to relate the RR model initial conditions with different external indicators of SM estimated by in situ, satellite and modelled data (Brocca et al., 2009a, b, 2011a; Tramblay et al., 2010, 2011, 2012; Beck et al., 2010; Coustau et al., 2012). In situ data were employed in many studies investigating the relationship between SM and runoff (e.g. Penna et al., 2011; Matgen et al., 2012) thus indirectly determining their potential use for RR modelling. Brocca et al. (2009a, 2011b) and Beck et al. (2010) used the SM products from ASCAT and AMSR-E for RR modelling in Italy, Luxembourg and Australia. However, the main purpose of these studies was to investigate the relationship between modelled and observed antecedent wetness conditions, without explicitly building a model that incorporates external SM data.

On these bases, a simplified continuous RR modelling approach is proposed in this study. Specifically, an event-based RR model able to use external SM information as input data is developed. This modelling approach shows the advantages of event-based RR models (reduced data and computational requirements, limited number of parameters to be estimated, simplicity in application) but at the same time overcomes the issues related to the selection of the SM initial condition. Therefore, the performance of this RR modelling approach significantly relies on the accuracy of the SM indicator used as input data. In this study, besides the description of the simplified continuous RR model, different SM indicators are compared in terms of flood hydrographs prediction. A small catchment in Greece (Rafina river basin, 109 km^2) is selected as a case study. In fact, for this catchment an early warning system for floods and fire risk management is going to be developed within the FLIRE project "FLoods and fIre Risk assessment and managEment", a project co-financed by European Commission General Directorate for the Environment, LIFE financial instrument with 50 %.

2 Study area and datasets

2.1 Rafina catchment

The study area is the Rafina river basin upstream the Rafina gauged section (109 km^2). This is a periurban area in the greater southeast Mesogeia region in Eastern Attica, Greece (Fig. 1). The area geographically extends from east of Hymettus mountain to the coastline of Evoikos Gulf. The mean altitude of the region is 227 m a.s.l. (with the minimum altitude being 0 and the maximum 909 m a.s.l.). Ground slope ranges from 0 to 37.8 % with a mean value of 7.5 %. Increased slopes and irregular terrain exist mainly at the upstream parts of the area.

Attica has a typical subtropical Mediterranean climate, with prolonged hot and dry summers succeeded by considerably mild and wet winters. The mean annual precipitation is approximately 400 mm, while snowfall is rare. Drought periods usually begin in May and last until October. The daily mean temperature ranges between 27° C during the summer months and 11° C during the winter months (Papathanasiou et al., 2013).

Geologically, the study area is part of the Attico–Cycladic Massif. Two main units dominate in the geological structure of Attica: (a) the crystalline basement (Palaeozoic–Upper Cretaceous), and (b) the Neogene–Quaternary clastic deposits. The basement consists of schists and carbonate rocks. The Neogene and Quaternary deposits fill up both the degradations and tectonic grabens of the East Attica basin and consist of marly limestones, marls, clays, sandstones, conglomerates and other coarse, unconsolidated sediments (Jacobshagen V., 1986).

Rafina catchment is covered by different and often conflicting land uses. More specifically, it includes forests (∼ 30 %), arable soils and grasslands (∼ 50 %) mainly located upstream and urban cells (∼ 20 %) located downstream (Alonistioti D., 2011). The study area is under constantly increasing urbanization, its northern part is forested with flammable material and sediment load transfer and soil erodibility are intense (Papathanasiou C. et al., 2009, 2011, 2012). The study area is particularly prone to both flash floods and forest fires and also vulnerable to their combined impact.

2.2 Hydro-meteorological data

The Laboratory of Hydrology and Water Resources Management of the School of Civil Engineers of the National Technical University of Athens (NTUA) operates the Hydrological Observatory of Athens (HOA), a dense monitoring hydrometeorological network in the greater Athens area. HOA is the evolution from the METEONET network that has been operating since 2005 and consists of 13 active meteorological stations and 4 active flow measuring stations, properly located in the area. The stations are equipped with sensors that measure with 10-minutes-temporal-resolution environmental parameters of hydrometeorological interest (https://hoa.ntua.gr). Parallel to that, the National Observatory of Athens (NOA) also operates a dense meteorological network in the greater Athens area recording valuable meteorological information also in ten-minutes-temporal resolution (NOA, 2012, www.meteo.gr/meteosearch).

Rainfall data selected for this study were extracted from Penteli, Pikermi, R400, R600 stations of HOA network, and, Kantza and Spata stations of NOA network (Fig. 1). Temperatures were retrieved from Pikermi thermometer. Note that, except for Penteli station – 2 km north outside of the catchment – all the stations are located within the catchment boundaries. Measured stages at Rafina gauged site were used to develop updated rating curves and thus evaluate discharges at the locations of the gauges. The period of analysis ranges from 12 March 2009 to 7 December 2012. The main data analysis included a quality control to remove inconsistent values, and aggregation operations to produce hourly based time step temporal resolution.

The rating curve developed for the Rafina site was based on velocity measurements carried out occasionally from the end of 2009 from low to medium water levels. It was assumed that (i) the instrument always worked in ideal conditions (as we realized from the discharge dataset), and, (ii) the geometry of gauging cross-section was stable in time, even though some changes may have been occurred during high flood events due to erosion, sediment transport and deposition.

Mean areal rainfall was calculated by the Thiessen polygon method whereas direct runoff was evaluated as in Melone et al. (2002) by using an appropriate baseflow separation technique.

For this study the events were extracted by selecting those with a continuous rainfall characterized by a total rainfall larger than 10 mm, and, no rainfall in the preceding one day . Eventually, fifteen rainfall runoff events were analysed with cumulated rainfall and runoff coefficients ranging from 12.3 to 87.5 mm and from 0.01 to 0.12, respectively (Table 1). For the most significant event – occurred on 3 February 2011 – the maximum recorded peak discharge was 39.5 $\mathrm{m^3\,s^{-1}}$ while for the selected flood with the lower intensity – recorded on 10 January 2012 – a peak discharge of 2.5 $\mathrm{m^3\,s^{-1}}$ was observed.

2.3 Soil moisture indicators

Four different SM indicators were selected covering the period 2009–2012. In particular, the selected indicators were: (i) ground SM obtained from measurements carried out at depth of 25 cm; (ii) ASCAT derived SM product (Wagner et al., 1999); (iii) AMSR-E derived SM product (Owe et al., 2001) and (iv) ERA-Land SM product from the ECMWF (Balsamo et al., 2012).

2.3.1 Ground soil moisture data

SM data selected for this study were collected at Pikermi station (see Fig. 1) that is the only station measuring SM data inside the catchment boundaries. The station was installed at the beginning of 2009 from HOA. The sensor measures volumetric SM at a depth of 25 cm through Frequency Domain Reflectometry (FDR) technique. The measurements were scheduled from March 2009 with ten minute temporal resolution.

2.3.2 ASCAT soil moisture product (Technical University of Wien, TU-Wien)

ASCAT is a real-aperture radar instrument on board the MetOp satellite. It measures radar backscatter at C-band (5.255 GHz) in VV polarization. Its spatial resolution is 25 km then re-sampled at 12.5 km. In the study area, measurements are available at least once a day (07:00–08:00 UTC in descending orbit and/or 18:00-20:00 UTC in ascending orbit).

The surface SM product (equivalent to a depth of 2–3 cm of the soil) is calculated from the backscatter measurements through a time series-based change detection approach previously used for the ERS-1/2 by Wagner et al. (1999). The SM is derived by selecting the historical lowest and highest backscatter measurement to which is assigned 0 % (dry), and 100 % (wet) reference, respectively. The ASCAT surface SM product used for this study covers the period 2009–2012 considering both ascending and descending overpass.

2.3.3 AMSR-E soil moisture product (UvA-NASA)

The AMSR-E sensor is the instrument on-board the NASA's Aqua satellite. It is a passive microwave radiometer measuring at 6.9 GHz (C-Band) and five higher frequencies. The sensor has provided measurements from May 2002 to October 2011 with daily ascending and descending overpasses. Its swath with is 1445 km.

In this study the Land Parameter Retrieval Model (LPRM) was used as a retrieval algorithm (Owe et al., 2001, 2008) on data of the period 2009–2011 (AMSR-E sensor stopped working in October 2011). The LPRM was developed by the University of Amsterdam (UvA) and NASA and was successfully tested over many sites in Europe (Brocca et al., 2011c).

2.3.4 ERA-Land soil moisture product (ECMWF)

The ECMWF provides medium range global forecasts for some environmental variables that include soil temperature, evaporation and SM. The ERA-Land SM produced by ECMWF is a land product developed at ECMWF exploiting most recent land modelling advancements, e.g. H-TESSEL Land Surface Model (Balsamo et al., 2012; Albergel et al., 2012). The SM analyses range from 1 January 1979 to 31 December 2012 and are available for 00:00, 06:00, 12:00 and 18:00 UTC with a spatial resolution of about 80 km (T255) considering 4 layers of soil (0–7, 7–29, 29–100 and 100–289 cm). In this study, the SM values relative to the first two layers (0–29 cm) were compared with in situ data, while the values of the first three soil layers (0–100 cm) were used for the RR transformation.

3 Methods

3.1 Simplified continuous rainfall runoff model

Continuous RR models simulate SM to take the variability of the wetness conditions prior to a rainfall event into account. If SM at the beginning of an event is provided by an external indicator, i.e. in situ or globally available SM observations such as satellite and model-based reanalysis SM products, the structure of a simplified but continuous RR model can be derived as schematized in Fig. 2.

The event-based RR model considered in this study employs the Soil Conservation Service – Curve Number (SCS-CN) method for estimation of losses. The choice of the SCS-CN method is due to its wide use since 1980 (Kim and Lee, 2008) and its simplicity. In particular, for a storm the partitioning of rainfall into runoff using the SCS-CN method is based on the following equation:

$$Q = \frac{(P - F_\mathrm{a})^2}{P - F_\mathrm{a} + S} P \geq F_\mathrm{a} \tag{1}$$

where F_a is the initial abstraction, S is the soil potential maximum retention, Q is the direct runoff depth, and P is the rainfall depth. The quantity F_a is considered linearly dependent on S by:

$$F_a = \lambda S \tag{2}$$

where λ is the initial abstraction coefficient. Equation (1) is extended for the time evolution of the effective rainfall rate, $e(t)$, within a given storm as (Melone et al., 2001):

$$e(t) = \frac{\mathrm{d}Q}{\mathrm{d}t} = \frac{p(t)(P(t) - F_a)(P(t) - F_a + 2S)}{(P(t) - F_a + S)^2} \quad P(t) \geq F_a \tag{3}$$

where p is the rainfall rate and $P(t) = \int_0^t p(\tau)\mathrm{d}\tau$.

If the standard SCS method is used, S is estimated based on dimensionless CN calculated as a function of land use, hydrological soil group, and total precipitation of previous 5 days, API_5 (Soil Conservation Service, 1993):

$$S = 25.4\left(\frac{1000}{\mathrm{CN}} - 10\right) \tag{4}$$

API_5 tries to reproduce the wetness state of the catchment by evaluating the cumulative rainfall of the preceding five days. However, as shown by (Brocca et al., 2009a, b; Tramblay et al., 2010) for several Mediterranean catchments, this approach is not adequate and the use of different indicators for SM was advocated.

Based on that, the simplified continuous RR model proposed here uses SM indicators provided by external sources (e.g. satellite data) to infer the value of S parameter for runoff determination. The RR model exploits the observed linear behaviour between the wetness state of the soil and the parameter S (Brocca et al., 2009a, b) by the following linear relationship:

$$S = a(1 - \theta_e) \tag{5}$$

In Eq. (5) θ_e is the relative SM (or degree of saturation) and a is a parameter to be estimated.

Once the time evolution of effective rainfall is computed, the routing to the outlet of the catchment is obtained by the convolution of the rainfall excess and the Geomorphological Unit Hydrograph (GIUH), such as proposed by (Gupta and Waymire, 1980). In the model the lag time is evaluated through the relationship proposed by (Melone et al., 2002):

$$L = \eta 1.19 A^{0.33} \tag{6}$$

with L being the lag time (h), A the area of the catchment (km^2), and η a parameter to be calibrated (Moramarco et al., 2005).

In synthesis, the simplified continuous RR model proposed in this paper uses the SM and the event rainfall data (i.e. continuous rainfall time series are not needed) as input data to simulate hourly flood hydrograph. Since the SM is provided by an external indicator, the $S-\theta_e$ relationship becomes a model relation embedded in the model structure and it is used to estimate the value of $S$for the analysed events. The calibration of the model involves only three parameters: the coefficient of initial abstractions λ, the parameter a of the $S-\theta_e$ relationship and the parameter of the lag time-area relationship.

For this study, a lumped model is employed even though the same concept can be easily applied to spatially distributed models. Finally, we underline that the different component of the models (i.e. SCS-CN and GIUH) can be changed while keeping the general model structure shown in Fig. 2.

3.2 Exponential filter

Root-zone SM data is the main control parameter on the catchment response to a given storm event. As a result, the knowledge of a very thin surface layer (ca. 0–5 cm) from remotely sensed SM products is not sufficient for hydrological applications concerning RR transformations.

To obtain the root-zone SM product (SWI, Soil Water Index) from the satellite-based surface observations, the semi-empirical approach developed by Wagner et al. (1999) is adopted. The approach is also known as Exponential filter and uses a single parameter T (characteristic time length) that represents the time scale of SM variation to obtain the SWI. The reader can find a more detailed description of this approach in Wagner et al. (1999) and Albergel et al. (2012).

3.3 The soil water balance model

Besides the use of SM data from in situ, satellite and global models, a Soil Water Balance (SWB) model driven by ground data observed in the study area is employed for the initialization of the event-based RR model, as in the classical schemes of continuous RR models (Brocca et al., 2011c). The SWB model is a simple bucket model representing the main processes needed for SM simulation (infiltration, percolation, evapotranspiration). More specifically, the processes are represented for infiltration through the Green-Ampt equation, for drainage by a gravity driven non-linear relationship and for actual evapotranspiration by a linear relationship with the potential evapotranspiration, calculated through a modified Blaney and Criddle method. The reader is referred to (Brocca et al., 2008, 2013) for the full description of the model equations and parameterisation. It should be underlined here that five physically-based parameters have to be estimated: maximum water capacity of the soil layer, saturated hydraulic conductivity, wetting front soil suction head, pore size distribution index and a correction parameter for potential evapotranspiration.

3.4 Performance scores

The Nash-Sutcliffe efficiency coefficient, NS, was used to evaluate the agreement between the simulated and observed hydrographs for each of the selected flood events

(Table 1):

$$\mathrm{NS} = 1 - \frac{\sum_{t=1}^{T_{\mathrm{ev}}} (Q_{\mathrm{obs}} - Q_{\mathrm{sim}})^2}{\sum_{t=1}^{T_{\mathrm{ev}}} (Q_{\mathrm{obs}} - \overline{Q}_{\mathrm{obs}})^2} \tag{7}$$

where Q_{obs} and Q_{sim} are the observed and simulated discharges at time t, $\overline{Q}_{\mathrm{obs}}$ is the mean value of the observed discharge during the event and T_{ev} is the event duration. In particular as objective function the mean of the NS calculated for each event, was selected and an hourly time step is used in the simulations. A gradient-based method is adopted as optimization algorithm.

In addition, to evaluate the performance of the model in reproducing flood events, the percentage error on peak discharge:

$$E_{Q_\mathrm{p}} = 100 \frac{\max(Q_{\mathrm{obs}}) - \max(Q_{\mathrm{sim}})}{\max(Q_{\mathrm{obs}})} \tag{8}$$

and on direct runoff volume

$$E_\mathrm{v} = 100 \frac{\sum_{t}^{T_{\mathrm{ev}}} Q_{\mathrm{obs}} - \sum_{t}^{T_{\mathrm{ev}}} Q_{\mathrm{sim}}}{\sum_{t}^{T_{\mathrm{ev}}} Q_{\mathrm{obs}}} \tag{9}$$

were both evaluated. The correlation coefficient, R, and the root mean squared error, RMSE, were used as performance scores in the comparison of the SM estimates (Sect. 4.1).

4 Results and discussions

4.1 Comparison of the soil moisture indicators

Figure 3 plots the relative, i.e. normalized between 0 and 1, SM temporal pattern for the SM indicators selected for this study in the period March 2009–December 2012. In particular, the relative values of the ground SM ($\text{SM}_{\text{in situ}}$) obtained from measurements carried out at depth of 25 cm, were compared with (i) simulated SM calculated by the SWB model, SM_{mod} (Fig. 3a), (ii) ERA-LAND SM product from ECMWF, obtained by the weighted mean of the 0–7 cm and 7–29 cm soil layers, (Fig. 3b), (iii) ASCAT derived SWI product (Fig. 3c) and (iv) AMSR-E derived SWI product (Fig. 3d).

In Fig. 3a, SM_{mod}, was obtained by the calibration of the SWB model on the ground SM at a depth of 25 cm by minimizing the RMSE in the period March 2009–December 2012. The SWB model performance was found satisfactory with $\text{RMSE} = 0.095$ and $R = 0.926$. As expected, the other modelled product, ERA-Land (Fig. 3b), provides lower performance ($R = 0.760$) likely due to its coarse spatial resolution (~ 80 km) and to errors in the meteorological forcing (mainly precipitation) that are obtained directly from the global model (not from ground observations as for the SWB model).

For remotely sensed SM indicators (Fig. 3c and d) the evaluation of SWI data was performed by varying the T parameter of the exponential filter from 1 to 200 days. For the ASCAT SWI, an anomalous behaviour was observed in dry periods which involved an anomalous increase without the occurrence of rainfall (see shaded areas in Fig. 3c). Such behaviour has been observed in other arid and semi-arid regions as well, and it is hypothesized to be due to volume scattering effects from dry sub-surface soil layers (Wagner et al., 2013). Given that to date there is no solution to this problem, the analysis was carried out twice by considering the whole dataset and the one with removed anomalous data. The calibration of the parameter T in the first case yielded $T = 133$ days with a correlation coefficient $R = 0.668$, while, when anomalous data were removed, $T = 21$ days and $R = 0.817$ were obtained. While the first result conflicts with the results of Wagner et al. (1999), Ceballos et al. (2005) and Brocca et al. (2011), the second one is in accordance with the studies of Wagner et al. (1999) which found $T = 20$ days for an area of about 600 000 km^2 in Ukraine. Therefore, in what follows, the ASCAT data set without anomalous data were considered. For the AMSR-E SWI product, (Fig. 3d) the calibration gave $T = 7.5$ days with $R = 0.844$. In this case, the lower values of T are due to the smother behaviour of the AMSR-E SM product with respect to ASCAT.

4.2 Event based rainfall-runoff modelling

4.2.1 Floods simulation by using “observed” initial conditions

As a first analysis, to assess the optimal antecedent wetness condition for the selected events, the “observed” soil potential maximum retention, S_{obs}, was determined by using observed rainfall and direct runoff depth by inverting Eq. (1):

$$S_{\text{obs}} = \frac{1}{2\lambda^2}\left(2\lambda P - \lambda Q + Q - \sqrt{\lambda^2 Q^2 - 2\lambda Q^2 + 4\lambda PQ + Q^2}\right) \quad (10)$$

Then, the two remaining model parameters, λ and η were calibrated by maximizing the mean of the NS values estimated for each event. The value of the parameters obtained in the calibration (Table 2) were $\lambda = 0.0015$ and $\eta = 0.669$ while S_{obs} ranges from 254 to 1188 mm (see Table 3) indicating a wide range of initial conditions at the beginning of the events. NS values range from 0.23 to 0.84, with a mean value of 0.60, indicating a quite satisfactory fit of the model, with the three greatest events (peak discharge $> 12\,\text{m}^3\,\text{s}^{-1}$) showing the highest NS values (NS > 0.80). The observed and simulated discharge hydrographs are shown in Fig. 4.

Due to the low reliability of the estimated rating curve as well as the weak response of the catchment to rainfall inputs in terms of runoff, for low magnitude flood events, the peak discharges are usually overestimated (Fig. 4). Indeed, a successful application of whatever rainfall runoff model to this area may be very difficult since the contribution of the rainfall to runoff is very small (see the low runoff coefficients in Table 1). The simulations with the "observed" initial conditions represent the best performance that can be attained by the employed event-based RR model in the Rafina catchment.

4.2.2 Floods simulation by using constant initial conditions

If an event-based RR model is run without the knowledge of the initial SM conditions, a constant value for all the events has to be selected. For that, the initial condition was set by using the average of the CN values computed by inverting Eq. (4), in which S for each event, was assumed equal to the S_{obs} obtained in the previous section and shown in Table 3. This simulation serves to assess the performance obtained by considering unknown and constant initial conditions (even though obtained from the S_{obs} values). Results of the calibration for λ and η parameters are given in Table 2. In this case, a very low performance was obtained with a mean and median NS value equal to −0.41 and 0.10, respectively (Table 3).

4.3 Simplified continuous rainfall runoff modelling

To assess the capability of the proposed simplified continuous RR model, the calibration was carried out in two different ways: first, by considering the whole flood dataset, then, by splitting the dataset in a calibration and a validation period. Normally, the soil layer depth that controls the RR transformation is usually larger than 25 cm. As a result, for the runoff modelling the parameters of the SM indicators presented in Sect. 4.1 were re-calibrated to give the best results in terms of runoff prediction by using only discharges recorded at Rafina gauged site. That is, the SWB model parameters, the T value for the ASCAT and AMSR-E products and the soil layers for the ERA-Land product were optimized along with the other parameters of the proposed model.

4.3.1 Model performance (calibration)

The results of the calibration using in situ data give NS values ranging from 0.16 to 0.85 with a mean of 0.44 ($\mathrm{NS}_{\text{in situ}}$ column in Table 3). Median E_{Q_p} shows the largest value among the other calibration results (see Fig. 5). When modelled SM of the SWB was used, very similar results were obtained with NS varying from 0.07 to 0.81 and a mean value equal to 0.45. In this case, the modelled SM obtained by calibrating the SWB model on the observed discharges (not shown for brevity) showed smoother variations in time with respect to the one in Fig. 3a (calibrated considering ground data).

For ERA-LAND SM, NS ranges from 0.13 to 0.86 with a mean of 0.49 ($\mathrm{NS}_{\mathrm{Era}}$ column in Table 3). In contrast with the results shown in Fig. 3b, the SM was calculated by considering the weighted mean of the three SM available layers (0–7, 0–29, 0–100 cm) because it supplied better results with respect to the first two layers.

For ASCAT, only the dataset with anomalous data removed was used in calibration, while, AMSR-E results do not account the two last events (19 December 2011 and 10 January 2012) because of the unavailability of SM product in these two dates. Table 3 shows results for ASCAT and AMSR-E. NS yielded 0.45 and 0.47 (mean) and 0.32 and 0.42 (median), respectively. Performances in volume and in peak discharge are very similar for both products. For ASCAT, the calibration was also carried without excluding anomalous data, leading to worse results for all the performance scores (not shown for brevity).

Note that in this case, the calibrated values of T (162.4 and 101.8 days for ASCAT and AMSR-E respectively) are much higher than the ones found in Sect. 4.1. These results are consistent with previous ones which highlight an influence of a deep soil layer in the RR transformation process (Brocca et al., 2010).

In the end, in terms of mean NS, the performance scores are encompassed in the ones obtained in by using S_{obs}, and those considering a constant CN. Although only 35 % of the events show NS greater than 0.6, the best results are obtained for the largest events (e.g. 11 December 2009, 3 February 2011, 24 February 2011) which are more significant for flood forecasting purposes. Figure 5a and b display the cumulative frequency in volume and absolute error in peak discharge, respectively. As expected, best results in E_v are obtained with the calibration using S_obs, while the calibration assuming a constant CN shows E_v greater than 100 % for the 15 % of the events. By contrast, using a constant CN seems to give good results in terms of E_{Q_p}. However, such a behaviour concerns only the smaller events. That is, the error rapidly increases over the one obtained with the simplified continuous RR model for the most significant events.

When using the continuous simplified RR model, ERA-LAND SM product obtains the best performance in terms of median NS (Table 3) and median of error in peak discharge E_{Q_p} (45.3 %, Fig. 5b). The ground data, which are based on soil moisture measurements at a depth of 25 cm, yield similar behaviour with respect to the other indicators both in terms of mean NS and E_v (Fig. 5a), but worse results in terms of median E_{Q_p} (Fig. 5b). If the calibration using ground data is carried out to take into account the soil layer depth influence on the RR transformation by varying the parameter T (not shown here for brevity), T yields 13.9 days with an improvement of the results in median NS from 0.39 to 0.43, and a reduction in median E_{Q_p} from 0.6 to 0.52.

The two remotely sensed SM products perform very similar although AMSR-E shows better results in terms of mean NS and E_{Q_p}. However, a direct comparison cannot be accomplished since the number of events used is not the same. When the latter two events are removed from ASCAT calibration, the latter slightly outperforms AMSR-E both in terms of mean and median NS.

4.3.2 Model performance (calibration and validation)

Despite the low number of events available, a simple split sample test procedure was performed by calibrating the model on the first eight events, then, the validation was executed on the remainder of them. The value of the parameters obtained in calibration is very similar to those shown in Table 2, and hence, it is not shown for brevity.

The validation was performed on seven events occurred from 24 February 2011 to 10 January 2012. Results in terms of mean NS are shown in Table 4. For AMSR-E the latter two events were not available, therefore, the validation involved only five events occurred from 24 February 2011 to 12 June 2011 (numbers in brackets in the validation column of Table 4 refer to the mean NS calculated on this period). Figure 6 6 plots the cumulative frequency of NS obtained in validation. Apart from the results of AMSR-E (based on five events where the model behaves better), the best performances are obtained for ERA-LAND, both in calibration and validation. The two satellite products perform very similar when choosing the same events and the results are comparable with those obtained with the SWB data. When using a constant S, instead of estimating it from the soil moisture indicator, the model performances (not shown) are very low with negative Nash values and large E_{Q_p}.

Figure 7 shows the observed and predicted hydrograph for the validation event of 24 February 2011 obtained by observed, modelled and ERA-LAND SM indicators (a), and by ASCAT and AMSR-E SM products (b). The results are fairly similar with ERA-Land and AMSR-E outperforming the other indicators in terms of NS ($\mathrm{NS} = 0.82$) and in E_{Q_p} (14 and 15 %, respectively). Lower performances are obtained for ASCAT ($\mathrm{NS} = 0.64$, $E_{Q_\mathrm{p}} = 37\,\%$) and ground data ($\mathrm{NS} = 0.69$, $E_{Q_\mathrm{p}} = 31\,\%$).

5 Conclusions

A simplified continuous RR model has been developed to simulate discharge hydrographs in a small Greek catchment located in Attica region. The model uses globally available soil moisture and event rainfall data (i.e. continuous rainfall time series are not needed) to simulate hourly flood hydrographs. The soil moisture provided by an external indicator is used to infer the initial condition of the model through a linear relationship previously introduced by Brocca et al. (2009a, b) directly embedded in the model structure. This modelling approach shows the advantages of event-based RR models but also overcomes the issues related to the selection of the soil moisture initial condition.

Different SM indicators are compared in terms of flood hydrographs prediction (ERA-LAND, ASCAT, AMSR-E, in situ and modelled data). In general, the model satisfactorily reproduced the flood events although the uncertainties present in the available rating curve. A soil layer thickness greater than 20–30 cm seems to control the rainfall runoff transformation process for the investigated basin. The best results were obtained when using the ERA-LAND SM product of ECWMF (0–100 cm). ASCAT and AMSR-E satellite soil moisture products perform very similar obtaining results comparable of those obtained by the SWB, which requires rain and temperatures measured in continuous. The model robustness was also tested by a split sample test procedure. The results were found good leading to the same general conclusions i.e. ERA-LAND performs better with respect to the other indicators.

For ASCAT, an anomalous behaviour was observed in dry periods, which involved an anomalous increase of the soil moisture without the occurrence of rainfall. Given that, the analysis for ASCAT was performed with removed anomalous data. This behaviour has already been observed in several arid and semi-arid regions and needs further investigation in future studies.

Overall, the similarity of the performance scores obtained by the global indicators such as ERA-LAND, ASCAT and AMSR-E with respect to the in situ and modelled data recommend the use of global available products to overcome the lack of ground data for hydrological applications in many areas of south Europe. Moreover, the small number of parameters used by the model along with the ever-increasing availability of global soil moisture retrievals, suggest a greater effort in research for the applicability of the model for flood forecasting purposes to poorly gauged sites of the Mediterranean areas. Future studies need to assess the performance of the model in other catchments to support these conclusions.

Acknowledgements. This research has been carried out under the Project FLIRE“FLoods and fIre Risk assessment and managEment”. The authors wish to thank NOA (National Observatory of Athens) and HOA (Hydrological Observatory of Athens) for providing the analyzed data for Rafina river basin, and, Gianpaolo Balsamo and Clément Albergel for providing soil moisture data of ERA-LAND.

References

Albergel, C., de Rosnay, P., Gruhier, C., Muñoz-Sabater, J., Hasenauer, S., Isaksen, L., Kerr, Y., Wagner, W.: Evaluation of remotely sensed and modelled soil moisture products using global ground-based in situ observations, Remote Sens. Environ., 118, 215–226, 2012.

Alonistioti, D.: Investigation of forest fire impact on the hydrological response of river basins in Eastern Attica region. Master Thesis, Inter-Departmental Postgraduate Course Water Resources Science and Technology, National Technical University of Athens, 2011 (in Greek).

Aronica, G. and Candela, A.: A Regional Methodology for Deriving Flood Frequency Curves (FFC) in Partially Gauged Catchments with Uncertain Knowledge of Soil Moisture Conditions, in: Proc. iEMSs 2004, University of Osnabru, Germany, 1147–1183, 2002.

Balsamo, G., Albergel, C., Beljaars, A., Boussetta, S., Brun, E., Cloke, H., Dee, D. Dutra, E., Pappenberger, F., de Rosnay, P., Muñoz Sabater, J., Stockdale, T., and Vitart, F.: ERA-Interim/Land: A global land-surface reanalysis based on ERA-Interim meteorological forcing. Era Report series: European Centre for Medium Range Weather Forecasts (ECWMF), 13, p. 25, 2012.

Barredo, J. I.: Major flood disasters in Europe: 1950–2005, Nat. Hazards, 42, 125–148, 2006.

Bartalis, Z., Wagner, W., Naeimi, V., Hasenauer, S., Scipal, K., Bonekamp, H, Figa, J., and Anderson, C.: Initial soil moisture retrievals from the METOP-A advanced Scatterometer (ASCAT), Geophys. Res. Lett., 34, L20401, doi:10.1029/2007GL031088, 2007.

Beck, H. E., de Jeu, R. A. M., Schellekens, J., van Dijk, A. I. J. M., and Bruijnzeel, L. A.: Improving Curve Number Based Storm Runoff Estimates Using Soil Moisture Proxies, Selected Topics in Applied Earth Observations and Remote Sensing, IEEE Journal of selected topics in applied earth observations and remote sensing, 2, 250–259, doi:10.1109/JSTARS.2009.2031227, 2009.

Beven, K.: A manifesto for the equifinality thesis, J. Hydrol., 320, 18–36, 2006.

Brocca, L., Melone, F., and Moramarco, T.: On the estimation of antecedent wetness conditions in rainfall – runoff modelling, Hyrol. Process., 642, 629–642, 2008.

Brocca, L., Melone, F., Moramarco, T., and Singh, V. P.: Assimilation of Observed Soil Moisture Data in Storm Rainfall-Runoff Modeling, J. Hydraul. Eng., 2, 153–165, 2009a.

Brocca, L., Melone, F., and Moramarco, T.: Antecedent Wetness Conditions based on ERS scatterometer data in support to rainfall-runoff modeling, J. Hydrol., 364, 73–86, 2009b.

Brocca, L., Melone, F., Moramarco, T., Wagner, W., Naeimi, V., Bartalis, Z., and Hasenauer, S.: Improving runoff prediction through the assimilation of the ASCAT soil moisture product, Hydrol. Earth Syst. Sci., 14, 1881–1893, doi:10.5194/hess-14-1881-2010, 2010.

Brocca, L., Melone, F., Moramarco, T., and Wagner, W.: "What perspective in remote sensing of soil moisture for hydrological applications by coarse-resolution sensors." in: Proc SPIE, Vol. 8174, edited by: Christopher, M. U., Neale and Antonino Maltese, 2011a.

Brocca, L., Melone, F., and Moramarco, T.: Distributed rainfall-runoff modelling for flood frequency estimation and flood forecasting, Hydrol. Process., 25, 2801–2813, 2011b.

Brocca, L., Hasenauer, S., Lacava, T., Melone, F., Moramarco, T., Wagner, W., Dorigo, W., Matgen, P., Martínez-Fernández, J., Llorens, P., Latron, J., Martin, C., and Bittelli, M.: Soil moisture estimation through ASCAT and AMSR-E sensors: an intercomparison and validation study across Europe, Remote Sens. Environ., 115, 3390–3408, doi:10.1016/j.rse.2011.08.003, 2011c.

Brocca, L., Melone, F., Moramarco, T., and Wagner, W.: A new method for rainfall estimation through soil moisture observations, Geophys. Res. Lett., 40, 853–858, doi:10.1002/grl.50173, 2013.

Camici, S., Tarpanelli, A., Brocca, L., Melone, F., and Moramarco, T.: Design soil moisture estimation by comparing continuous and storm-based rainfall-runoff modeling, Water Resour. Res., 47, W05527, doi:10.1029/2010WR009298, 2011.

Ceballos, A., Scipal, K., Wagner, W., and Martínez-Fernández, J.: Validation of ERS scatterometer-derived soil moisture data in the central part of the Duero Basin, Spain, Hydrol. Process., 19 1549–1566, doi:10.1002/hyp.5585, 2005.

Coustau, M., Bouvier, C., Borrell-Estupina, V., and Jourde, H.: Flood modelling with a distributed event-based parsimonious rainfall-runoff model: case of the karstic Lez river catchment, Nat. Hazards Earth Syst. Sci., 12, 1119–1133, doi:10.5194/nhess-12-1119-2012, 2012.

de Rosnay P., Drusch, M., Vasiljevic, D., Balsamo, G., Albergel, C., and Isaksen, L.: A Simplified Extended Kalman Filter for the Global Operational Soil Moisture Analysis at ECMWF, Q. J. Roy. Meteorol. Soc., 139, 1199–1213, doi:10.1002/qj.2023, 2013.

Dorigo, W. A., Wagner, W., Hohensinn, R., Hahn, S., Paulik, C., Xaver, A., Gruber, A., Drusch, M., Mecklenburg, S., van Oevelen, P., Robock, A., and Jackson, T.: The International Soil Moisture Network: a data hosting facility for global in situ soil moisture measurements, Hydrol. Earth Syst. Sci., 15, 1675–1698, doi:10.5194/hess-15-1675-2011, 2011.

Gupta, V. and Waymire, C.: A representation of an instantaneous unit hydrograph from geomorphology, Water Resour. Res., 16, 855–862, 1980.

IPCC: Climate Change 2001: Impacts, adaptation and vulnerability, Contribution of Working Group II to the Third Assessment Report of the Intergovernmental Panel on Climate Change, edited by: McCarthy, J. J., Canziani, O. F., Leary, N. A., Dokken, D. J., and White, K. S., Cambridge University Press, Cambridge, UK, and New York, USA, 2001.

Jacobshagen, V.: Geologie von Griechenland, Beiträge zur regionalen Geologie der Erde, Gebrüder Borntraeger, Berlin, 1986.

Kerr, Y. H., Waldteufel, P., Wigneron, J.-P., Delwart, S., Cabot, F., Boutin, J., Escorihuela, M.-J., Font, J., Reul, N., Gruhier, C., Juglea, S. E., Drinkwater, M. R., Hahne, A., Martin-Neira, M., and Mecklenburg, S.: The SMOS Mission: New Tool for Monitoring Key Elements ofthe Global Water Cycle, Proc. IEEE, 98, 666–687, doi:10.1109/JPROC.2010.2043032, 2010.

Kim, N. W. and Lee, J.: Temporally weighted average curve number method for daily runoff simulation, Hydrol. Process., 4948, 4936–4948, 2008.

Matgen, P., Heitz, S., Hasenauer, S., Hissler, C., Brocca, L., Hoffmann, L., Wagner, W., and Savenije, H. H. G.: On the potential of METOP ASCAT-derived soil wetness indices as a new aperture for hydrological monitoring and prediction: a field evaluation over Luxembourg, Hydrol. Process., 26, 2346–2359, doi:10.1002/hyp.8316, 2012.

Melone, F., Neri, N., Morbidelli, R., and Saltalippi, C.: A conceptual model for flood prediction in basins of moderate size, in: Applied simulation and modeling, edited by: Hamza, M. H., 461–466, California: IASTED Acta Press, 2001.

Melone, F., Corradini, C., and Singh, V. P.: Lag prediction in ungauged basins: an investigation through actual data of the upper Tiber River valley, Hydrol. Process., 16, 1085–1094. doi:10.1002/hyp.313, 2002.

Moramarco, T., Melone, F., and Singh, V. P.: Assessment of flooding in urbanized ungauged basins: a case study in the Upper Tiber area – Italy, Hydrol. Processe., 19, 1909–1924, 2005.

National Observatory of Athens (NOA): The network of automatic meteorological stations of the National Observatory of Athens, September 2012, available at: www.meteo.gr/meteosearch (last access: 5 May 2013), 2012 (report in Greek).

National Observatory of Athens (NOA): The network of automatic meteorological stations of the National Observatory of Athens, September 2012, available at: ww.meteo.gr/meteosearch (last access: 5 May 2013), 2012 (report in Greek).

Owe, M., De Jeu, R. and Walker, J.: A methodology for surface soil moisture and vegetation optical depth retrieval using the microwave polarization difference index, IEEE Trans. Geosci. Remote Sens., 39, 1643–1654, 2001.

Owe, M., De Jeu, R., and Holmes, T.: Multisensor historical climatology of satellite-derived global land surface moisture, J. Geophys. Res., 113, F01002, doi:10.1029/2007JF000769, 2008.

Papathanasiou, C., Safiolea, E., Makropoulos, C., and Mimikou, M.: The FLADAR Project and its contribution to the implementation of the EU Flood Directive 2007/60, Proc. 11th International Conference on Environmental Science and Technology, 3–5 September, Chania, Crete, Greece, 2009.

Papathanasiou, C., Alonistioti, D., Kasella, A., Makropoulos, C., and Mimikou, M.: The impact of forest fires on the vulnerability of peri-urban catchments to flood events (The case of the Eastern Attica region), Special Issue of the Global NEST Journal on Hydrology and Water Resources, September 2012, 14, 294–302, 2012.

Papathanasiou, C., Makropoulos, C., Baltas, E., and Mimikou, M.: The Hydrological Observatory of Athens: a state-of-the-art network for the assessment of the hydrometeorological regime of Attica, Proc. 13th International Conference on Environmental Science and Technology, 5–7 September, Athens, Greece, submitted, 2013.

Paquet, E., Garavaglia, F., Garçon, R., and Gailhard, J.: The SCHADEX method: A semi-continuous rainfall–runoff simulation for extreme flood estimation, J. Hydrol., 495, 23–37, doi:10.1016/j.jhydrol.2013.04.045, 2013.

Penna, D., Tromp-van Meerveld, H. J., Gobbi, A., Borga, M., and Dalla Fontana, G.: The influence of soil moisture on threshold runoff generation processes in an alpine headwater catchment, Hydrol. Earth Syst. Sci., 15, 689–702, doi:10.5194/hess-15-689-2011, 2011.

Soil Conservation Service (SCS): Hydrology, National Engineering Handbokk, Supplement A, Section 4, Washington, DC: Soil Conservation Service, USDA, 1993.

Tramblay, Y., Bouvier, C., Martin, C., Didon-Lescot, J.-F., Todorovik, D., and Domergue, J.-M.: Assessment of initial soil moisture conditions for event-based rainfall–runoff modelling, J. Hydrol., 387, 176–187, doi:10.1016/j.jhydrol.2010.04.006, 2010.

Tramblay, Y., Bouvier, C., Ayral, P.-A., and Marchandise, A.: Impact of rainfall spatial distribution on rainfall-runoff modelling efficiency and initial soil moisture conditions estimation, Nat. Hazards Earth Syst. Sci., 11, 157–170, doi:10.5194/nhess-11-157-2011, 2011.

Tramblay, Y., Bouaicha, R., Brocca, L., Dorigo, W., Bouvier, C., Camici, S., and Servat, E.: Estimation of antecedent wetness conditions for flood modelling in northern Morocco, Hydrol. Earth Syst. Sci., 16, 4375–4386, doi:10.5194/hess-16-4375-2012, 2012.

Van Steenbergen, N. and Willems, P.: Increasing River Flood Preparedness by Real-time Warning Based on Wetness State Conditions, J. Hydrol., 489, 227–237, doi:10.1016/j.jhydrol.2013.03.015, 2013.

Viviroli, D., Mittelbach, H., Gurtz, J., and Weingartner, R.: Continuous simulation for flood estimation in ungauged mesoscale catchments of Switzerland – Part II: Parameter regionalisation and flood estimation results, J. Hydrol., 377, 208–225, doi:10.1016/j.jhydrol.2009.08.022, 2009.

Wagner, W., Lemoine, G., and Rott, H.: A Method for Estimating Soil Moisture from ERS Scatterometer and Soil Data, Remote Sens. Environ., 4257, 191–206, 1999.

Wagner, W., Hahn, S., Kidd, R., Melzer, T., Bartalis, Z., Hasenauer, S., Figa, J., de Rosnay, P., Jann, A., Schneider, S., Komma, J., Kubu, G., Brugger, K., Aubrecht, C., Zuger, J., Gangkofner, U., Kienberger, S., Brocca, L., Wang, Y., Bloeschl, G., Eitzinger, J., Steinnocher, K., Zeil, P., and Rubel, F.: The ASCAT soil moisture product: specifications, validation results, and emerging applications, Meteorologische Z., 22,. 5–33, doi:10.1127/0941-2948/2013/0399, 2013.

Younis, J., Anquetin, S., and Thielen, J.: The benefit of high-resolution operational weather forecasts for flash flood warning, Hydrol. Earth Syst. Sci., 12, 1039–1051, doi:10.5194/hess-12-1039-2008, 2008.

Table 1. Main characteristics of the selected rainfall-runoff events.

Dates	Maximum discharge [$m^3 s^{-1}$]	Lag time [h]	Total rainfall [mm]	Direct runoff [mm]	Runoff coefficient [-]	Duration [h]
21 March 2009	3.5	2.9	14.6	0.3	0.02	22
25 October 2009	10.7	3.8	27.8	1.3	0.04	25
26 October 2009	4.0	3	12.3	0.3	0.03	19
3 November 2009	4.4	4.1	21.0	0.3	0.02	24
11 December 2009	12.4	4.0	34.8	1.8	0.05	24
2 January 2011	3.3	5.5	18.5	0.2	0.01	30
3 February 2011	39.5	5.4	87.5	10.7	0.12	40
18 February 2011	7.5	4.1	12.5	0.6	0.04	19
24 February 2011	18.8	5.2	47.2	5.8	0.12	37
7 March 2011	5.5	5.0	17.0	0.8	0.05	26
17 April 2011	2.9	4.1	12.7	0.2	0.02	23
26 April 2011	5.0	5.8	28.6	1.0	0.04	37
12 June 2011	9.3	4.4	28.2	1.1	0.04	19
19 December 2011	6.7	8.5	18.8	1.0	0.05	35
10 January 2012	2.5	9.2	15.0	0.7	0.05	39

Title Page
Abstract
Introduction
Conclusions
References
Tables
Figures
◀◀
▶▶
◀
▶
Back
Close
Full Screen / Esc
Printer-friendly Version
Interactive Discussion

Table 2. Calibrated parameters of the event based models by the maximization of the mean NS.

Soil moisture indicator	a [mm^{-1}]	η	λ	T [days]
S_{obs}		0.669	0.0015	–
In situ	1029	0.667	0.0010	–
Modelled	1107	0.663	0.0010	–
ERA-Land	1097	0.659	0.0010	–
ASCAT	1074	0.667	0.0010	162.4
AMSR-E	1200	0.648	0.0021	101.8
S_{cost}	–	0.307	0.0010	–

Table 3. NS performance of the event based models used in the study.

Dates	S_{obs} [mm]	NS	$NS_{in situ}$	NS_{mod}	NS_{Era}	NS_{ASCAT}	NS_{AMSR-E}	NS_{Scost}
21 March 2009	653.3	0.40	0.42	0.22	0.43	0.32	0.42	−0.62
25 October 2009	543.3	0.57	0.49	0.39	0.45	0.42	0.32	0.5
26 October 2009	372.0	0.35	0.18	0.10	0.13	0.10	0.02	0.28
3 November 2009	1051.2	0.68	0.48	0.67	0.53	0.61	0.68	−3.8
11 December 2009	599.1	0.84	0.82	0.78	0.86	0.84	0.73	0.58
2 January 2011	1187.5	0.64	0.31	0.46	0.62	0.27	0.25	−4.75
3 February 2011	612.5	0.80	0.82	0.81	0.77	0.82	0.80	0.75
18 February 2011	253.9	0.59	0.26	0.37	0.35	0.29	0.38	0.00
24 February 2011	330.4	0.84	0.85	0.79	0.80	0.73	0.83	0.75
7 March 2011	323.8	0.81	0.59	0.80	0.82	0.71	0.81	0.37
17 April 2011	646.5	0.23	0.16	0.19	0.16	0.24	0.09	−0.61
26 April 2011	718.9	0.77	0.78	0.69	0.66	0.78	0.47	0.53
12 June 2011	329.9	0.53	0.34	0.31	0.36	0.23	0.28	−0.12
19 December 2011	302.1	0.53	0.18	0.14	0.20	0.23	–	−0.17
10 January 2012	289.9	0.46	0.23	0.07	0.15	0.11	–	0.09
Mean	547.62	0.60	0.44	0.45	0.49	0.45	0.47	−0.41
Median	543.3	0.59	0.39	0.39	0.45	0.32	0.42	0.09
Max	1187.5	0.84	0.85	0.81	0.86	0.84	0.83	0.75
Min	253.9	0.23	0.16	0.07	0.13	0.1	0.02	−4.75

Table 4. Summary of the model performance in terms of Mean NS in calibration (8 events, from 21 March 2009–to 18 February 2011) and validation (7 events, from 24 February 2011 to 10 January 2011). Numbers in brackets in the validation column refer to the validation performed on 5 events, (the only available for AMSR-E).

	Calibration	Validation
Period	21 March 2009–18 February 2011	24 February 2011–10 January 2011
# events	8	(24 February 2011–12 June 2011) 7(5)
Score	Mean NS	Mean NS
In situ	0.48	0.34 (0.43)
Modelled	0.48	0.42(0.55)
ERA-Land	0.52	0.44 (0.56)
ASCAT	0.48	0.37 (0.48)
AMSR-E	0.47	(0.47)

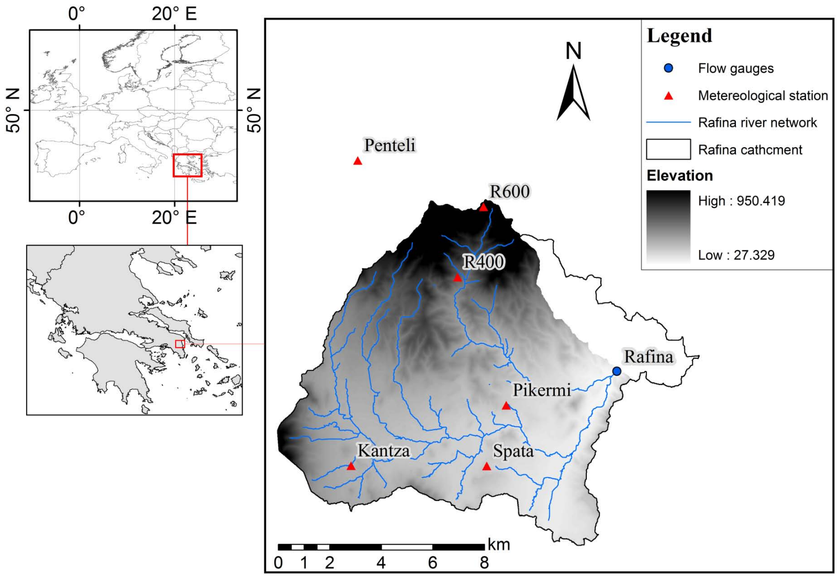

Fig. 1. Study area and locations of meteorological and flow gauging stations used in the study.

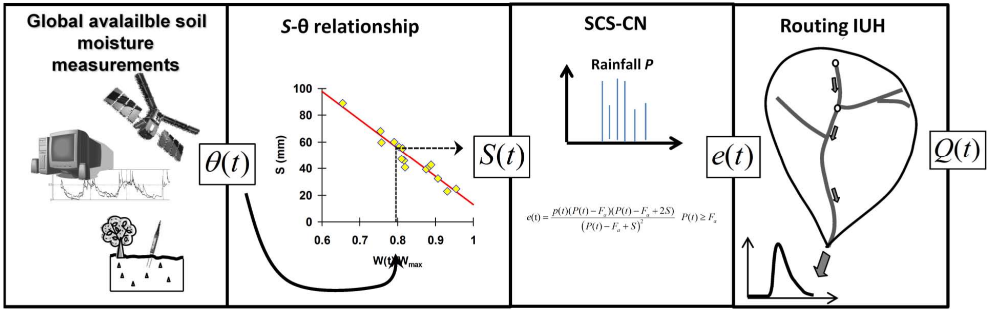

Fig. 2. Structure of the simplified continuous RR model.

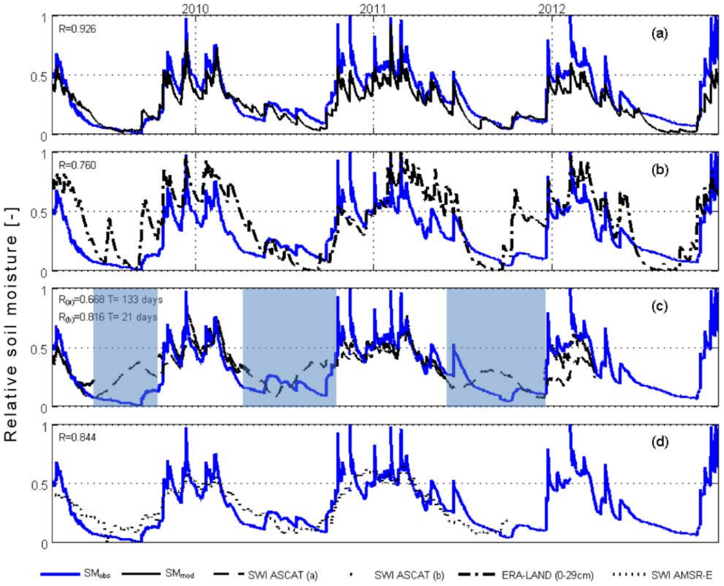

Fig. 3. Relative soil moisture temporal pattern for the different soil moisture indicators selected for this study (period March 2009–December 2012). Comparison between the relative values of the ground soil moisture obtained from measurements carried out at depth of 25 cm (Number of data, $N = 32\,783$ hourly data) with: **(a)** simulated soil moisture calculated by the SWB component ($N = 32\,783$), **(b)** ERA-Land soil moisture product from ECMWF obtained by weighted mean of the 0–7 cm and 7–29 cm products ($N = 1367$), **(c)** SWI ASCAT derived soil moisture product considering the whole dataset ($N = 1018$) (the shaded windows refer to the anomalous data in the dry periods) and the dataset with data in shaded windows removed ($N = 553$), **(d)** SWI AMSR-E derived soil moisture product ($N = 584$).

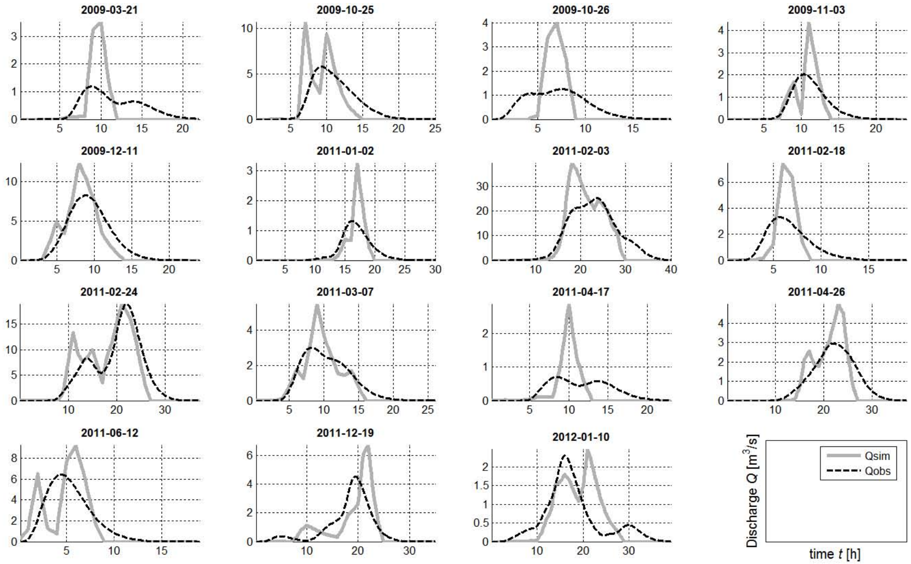

Fig. 4. Observed and simulated hydrograph with “observed” initial conditions for the selected flood events at Rafina gauged site.

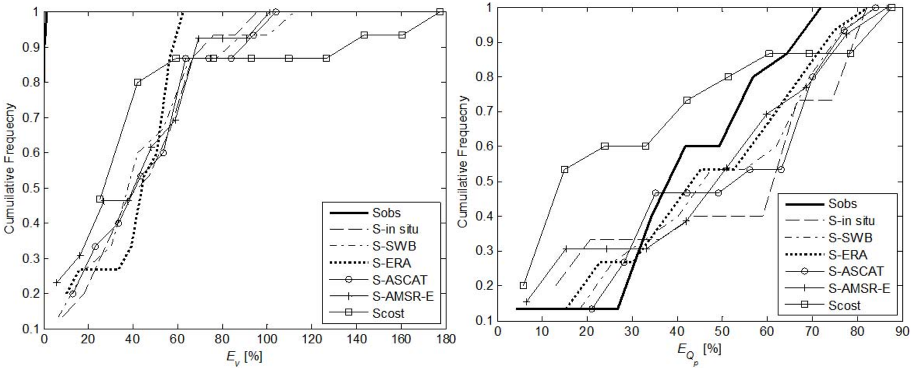

Fig. 5. Cumulative frequency of absolute error in Volume E_v **(a)** and absolute error in peak discharge, E_{Q_p} **(b)** calculated for the selected events.

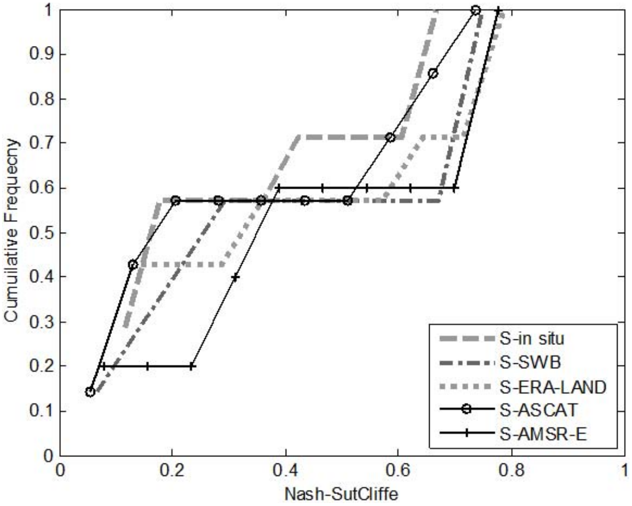

Fig. 6. Cumulative frequency of NS obtained in the validation period.

Title Page
Abstract
Introduction
Conclusions
References
Tables
Figures
◀◀
▶▶
◀
▶
Back
Close
Full Screen / Esc
Printer-friendly Version
Interactive Discussion

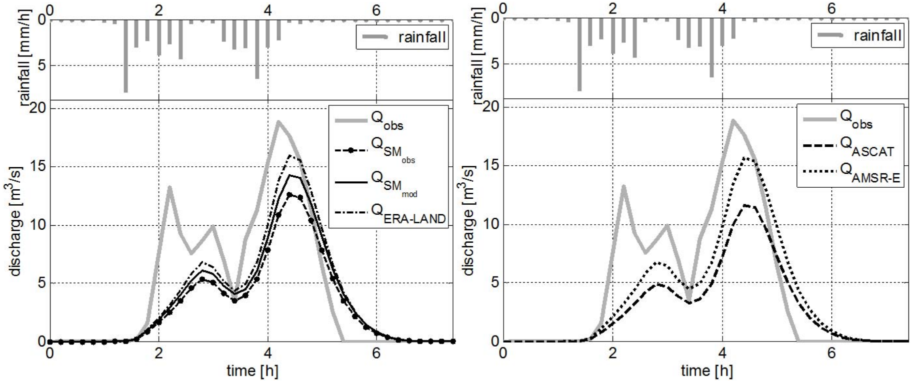

Fig. 7. Comparison of observed and predicted hydrographs for the validation event of 24 February 2011 at Rafina gauged site for ground SM, modelled SM and ERA-LAND SM **(a)**; ASCAT and AMSR-E **(b)**.